J. Fluid Mech. (1971), *vol.* 48, *part* 2, *pp.* 405–415
Printed in Great Britain

Inviscid instability of an unbounded heterogeneous shear layer

By S. A. MASLOWE† AND R. E. KELLY
School of Engineering and Applied Science, University of California, Los Angeles, California 90024

(Received 2 September 1970 and in revised form 25 January 1971)

Stability curves are computed for both spatially and temporally growing disturbances in a stratified mixing layer between two uniform streams. The low Froude number limit, in which the effects of buoyancy predominate, and the high Froude number limit, in which the effects of density variation are manifested by the inertial terms of the vorticity equation, are considered as limiting cases. For the buoyant case, although the spatial growth rates can be predicted reasonably well by suitable use of the results for temporal growth, spatially growing disturbances appear to have high group velocities near the lower cut-off wave-number. For the inertial case, it is demonstrated that density variations can be destabilizing. More precisely, when the stream with the higher velocity has the lower density, both the wave-number range of unstable disturbances and the maximum spatial growth rate are increased relative to the case of homogeneous flow. Finally, it is shown how the growth rate of the most unstable wave in the inertial case diminishes as buoyancy becomes important.

1. Introduction

The linear stability theory of heterogeneous shear flows has been of interest for many years, primarily due to its relevance to atmospheric and oceanic phenomena. For such flows, although the flow velocities are rather small, the Reynolds number is still quite large, and so an incompressible inviscid flow model would appear to be a reasonable one. The linearized versions of the equation of incompressibility and the vorticity equation can be combined to yield the governing stability equation, which is becoming known as the Taylor–Goldstein equation. From this equation, Miles (1961) and Howard (1961) have demonstrated that a sufficient condition for linear stability is that the local Richardson number, which is a ratio of the stabilizing effect of gravity to the destabilizing effect of shear, be everywhere greater than $\frac{1}{4}$. This result is true for the general case, when density variations occur in both the buoyant and inertial terms of the equations of motion.

As far as eigenvalues and eigensolutions for continuous profiles are concerned, however, detailed results have been restricted mainly to the case of neutral

† Present address: Department of Mathematics, Massachusetts Institute of Technology, Cambridge, Massachusetts 02139.

disturbances in the low Froude number limit, when the inertial effects of heterogeneity are neglected (cf. Drazin & Howard 1966; Thorpe 1969). One example, first discussed by Hølmboe, corresponds to a mixing-layer profile of the form

$$\bar{u}(y) = 1 + \tanh y, \quad \bar{\rho} = \exp(-\beta \tanh y), \tag{1.1}$$

where $\bar{u}$ and $\bar{\rho}$ are the mean non-dimensional velocity and density profiles and are functions of the dimensionless vertical co-ordinate y. Comparison of the shape of the above profiles with the experimental mixing-layer data of Scotti (1969) shows reasonable agreement, although Scotti's results actually concern flows in which the difference in velocity across the layer is much smaller than the mean velocity. This has no consequence for the temporal stability problem but does affect the amplification rates of spatially growing disturbances. Hazel (1969) has obtained results for temporally growing disturbances for the flow (1.1), as well as for various other flow configurations. Our results for spatially growing disturbances, which should correspond more closely to those observed experimentally in a wind tunnel, are intended to supplement his results. Maslowe & Thompson (1971) present stability curves at finite Reynolds numbers, in the low Froude number limit, for the flow (1.1). Their results indicate that the inviscid results should be meaningful for Reynolds numbers above, roughly, 200, although this depends upon the Richardson number (and also, perhaps, upon the process of linearization; for a discussion of the non-linear critical layer in stratified shear flows, see Kelly & Maslowe (1970)).

The large Froude number limit, in which buoyancy forces are negligible, is of some practical interest for certain propulsive applications, such as the gaseous core nuclear rocket engine employing the coaxial flow concept (McLafferty 1968). In this limit, a solution was obtained by Menkes (1959) for the flow

$$\bar{u}(y) = \tanh y, \quad \bar{\rho}(y) = \exp(-2\beta y). \tag{1.2}$$

Menkes found the stability boundary to be given by $c = -\beta$, $\alpha^2 + \beta^2 = 1$, where c and α are the neutral disturbance phase speed and wave-number, respectively, and $\alpha < 1$ for unstable disturbances. According to this result, the influence of density variation is stabilizing in the sense that as β increases, the range of unstable α decreases, and, for $\beta > 1$, the flow is stable. This result has been quoted on several occasions as indicating that the inertial variations of density are stabilizing. In reality, the result appears to be an anomalous one, peculiar to the assumed density profile which vanishes as $y \to \infty$. For a density profile which approaches a constant value as $y \to \pm\infty$, the Kelvin–Helmholtz model should govern the stability at low α, and this model predicts that the flow will be unstable in the absence of gravity. One therefore suspects that the conclusion of Menkes is misleading as far as more realistic flows are concerned. In fact, we shall see later that, for the flow described by (1.1), the inertial effects of density variation can actually be destabilizing. In contrast, it is interesting to remember that, for the buoyant case, Drazin (1958) obtained meaningful results regarding shear flow instability by use of the model given by (1.2).

Because the theorem of Miles and Howard predicts that the flow will become stable as the local Richardson number approaches $\frac{1}{4}$, we consider an intermediate

case in the concluding section in order to demonstrate how the growth rate of the wave which is most unstable at high Froude numbers decreases as the Froude number decreases.

2. Formulation and numerical procedure

We consider the stability of a horizontal parallel flow that is incompressible, but whose density varies in the vertical direction. In the linearized theory, we superimpose a small perturbation upon the mean flow, where the disturbance stream function ψ is of the form

$$\psi = \phi(y) \exp[i\alpha(x-ct)]. \tag{2.1}$$

For temporally varying waves, α is the real wave-number and c is a complex quantity whose real part is the wave speed. The density perturbation, which is represented in a similar manner, can be eliminated by combining the incompressibility and vorticity eqations. The resulting equation for ϕ can be written in the form (cf. Drazin & Howard 1966)

$$\phi'' - \alpha^2\phi - \frac{\bar{u}''}{\bar{u}-c}\phi + J_0 f' \frac{\phi}{(\bar{u}-c)^2} - \beta f' \left(\phi' - \frac{\bar{u}'}{\bar{u}-c}\phi\right) = 0, \tag{2.2}$$

where we have assumed a density variation of the form $\bar{\rho} = \exp\{-\beta f(y)\}$. The variables in (2.2) have been made non-dimensional with respect to a length scale L and characteristic velocity V. If g is the gravitational constant, the dimensionless parameter

$$J_0 = g\beta L/V^2 \tag{2.3}$$

is an overall Richardson number, while (J_0/β) is the reciprocal of the Froude number and

$$J(y) = J_0 f'/(\bar{u}')^2 \tag{2.4}$$

is the local Richardson number.

As $|y|$ becomes large, we assume that $\bar{u}$ and $\bar{\rho}$ become constant (c.f. 1.1). Hence, we have

$$\phi \sim e^{-\alpha y}, \quad \phi' \sim -\alpha\phi \quad \text{as} \quad y \to +\infty, \tag{2.5}$$

and

$$\phi \sim e^{\alpha y}, \quad \phi' \sim \alpha\phi \quad \text{as} \quad y \to -\infty. \tag{2.6}$$

In meteorological and oceanographical phenomena, $\beta \ll 1$ typically and $J_0 \sim O(1)$ so that the terms proportional to β can be neglected in (2.2). Hølmboe found in that limit the singular neutral mode

$$c = 1, \quad J_0 = \alpha(1-\alpha), \quad \phi = (\operatorname{sech} y)^{\alpha} (\tanh y)^{1-\alpha}, \tag{2.7}$$

corresponding to the mean flow profiles (1.1). Note that because the local Richardson number $J(y) = J_0 \cosh^2 y$ in Hølmboe's model, the minimum value of $J(y)$ is at the critical point, $y = 0$, where $\bar{u}(y) = c$.

When the density variation is moderate and occurs over a relatively small distance, and the velocity is reasonably high, we have the inertial limit characterized by $J_0 \ll 1$ and $\beta \sim O(1)$. For the moment, let us retain both buoyant and inertial terms so that the numerical procedure can be formulated on a general basis. The method we will employ has been used previously by Michalke (1965) in his study of a homogeneous mixing layer having the velocity profile (1.1).

To begin with, we introduce the transformation

$$\phi = \exp\left(\int_0^y \Phi\, dy\right) \tag{2.8}$$

which, after substituting into (2.2), leads to the Riccati equation

$$\Phi' = \alpha^2 - \Phi^2 + \frac{\bar{u}''}{\bar{u}-c} - \frac{J_0 f'}{(\bar{u}-c)^2} + \beta f'\left(\Phi - \frac{\bar{u}'}{\bar{u}-c}\right). \tag{2.9}$$

Next, we transform the independent variable to

$$Z = \tanh y, \tag{2.10}$$

thereby reducing the range of integration to $-1 \leqslant Z \leqslant +1$. Hølmboe's model, in terms of Z, is written as

$$\bar{u} = 1+Z, \quad \bar{u}' = f' = 1-Z^2, \quad \bar{u}'' = -2Z(1-Z^2). \tag{2.11}$$

When substituted into (2.9), equations (2.10) and (2.11) yield the desired form of the stability equation, namely

$$\Phi' = \frac{\alpha^2-\Phi^2}{1-Z^2} - \frac{2Z}{1+Z-c} - \frac{J_0}{(1+Z-c)^2} + \beta\left(\Phi - \frac{1-Z^2}{1+Z-c}\right). \tag{2.12}$$

The boundary conditions for Φ are, from (2.5) to (2.10),

$$\Phi(-1) = \alpha \quad \text{and} \quad \Phi(1) = -\alpha. \tag{2.13}$$

By employing L'Hôpital's rule and the above values for Φ, we find that the initial values for Φ', required for the numerical integration of (2.12), are

$$\Phi'(1) = -\left\{\frac{1}{1+\alpha}\right\}\left\{\frac{1}{1-\frac{1}{2}c} + \frac{J_0}{(2-c)^2} + \beta\alpha\right\} \tag{2.14}$$

and

$$\Phi'(-1) = \left\{\frac{1}{1+\alpha}\right\}\left\{\alpha\beta - \frac{2}{c} - \frac{J_0}{c^2}\right\}. \tag{2.15}$$

In the eigenvalue problem associated with (2.12)–(2.15), all but two of the various parameters can be specified independently. An iterative procedure is used to determine these constants. To apply this procedure, (2.12) is integrated inward from both $Z = +1$ and $Z = -1$, which, in general, leads to two different values of $\Phi(0)$. Only when the proper values have been used for the unspecified constants will both the real and imaginary parts of Φ match at $Z = 0$.

The numerical integration of (2.12) has been carried out using a Runge–Kutta procedure with a step size of 0·025. Double-precision, complex arithmetic was employed in making these calculations, the results of which are presented in the following sections of this paper.

3. The buoyant case

We first consider the limit $\beta \to 0$ and neglect the inertial terms in (2.12)–(2.15). The computation of stability curves for this case is simplified by the observation that, due to the antisymmetry of $\bar{u}$ and f, $c_r = 1$ in the temporal theory. In addition, the stability boundary for Hølmboe's model is already known. Therefore, the calculation of curves of constant growth rate, αc_i, is relatively straightforward.

The numerical results are shown in figure 1 along with the approximate curves calculated by Drazin & Howard (1961) for small α and J_0. Corresponding to each value of J_0, there is a wave-number for which the growth rate is a maximum. The locus of such points is indicated by the curve labelled α_M. The Drazin–Howard expansion predicts α_M adequately only for the higher values of J_0 (i.e. lower values of growth rate).

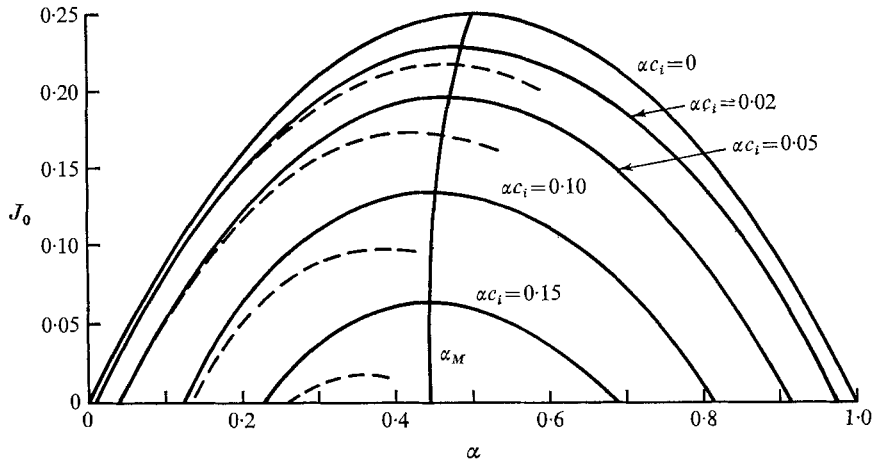

FIGURE 1. Curves of constant temporal growth rate in the buoyant case (α_M is the wave-number for maximum amplification). – – –, Drazin & Howard (1961).

The preceding development has been based upon the consideration of spatially periodic waves that can grow in time. However, in most experiments involving shear flows, unstable waves will actually grow in space rather than in time. The proper Fourier representation in that case is of the form

$$\psi = \phi(y) \exp[i(\alpha x - \omega t)], \tag{3.1}$$

where α is now complex and ω, the frequency, is real. The real part of α is the wave-number of the disturbance, whereas $-\alpha_i$ is the spatial amplification factor. To modify (2.12)–(2.15) for spatially growing waves, the quantity c is simply replaced by ω/α.

Let us now examine the numerical results for spatially growing waves. Using the iteration procedure discussed above, stability curves of constant growth rate ($-\alpha_i$), have been computed. These results are illustrated in figure 2. The wave-number for maximum growth is always somewhat less than that occurring in the temporal case.

Because the waves are no longer spatially periodic, $c_r \neq 1$, in general. The dispersive character of waves that grow in space is illustrated by the curves of c_r *vs.* α_r in figure 3. As pointed out by Michalke, the greatest variation in the phase speed occurs at the lower frequencies, but it is clear that the variation is qualitatively different from stratified flow. Indeed, $\partial c_r/\partial \alpha_r$, and therefore the group velocity, is very large near the lower cut-off wave-number (this can also be seen easily from the Kelvin–Helmholtz dispersion relation by allowing α to approach the cut-off wave-number from below).

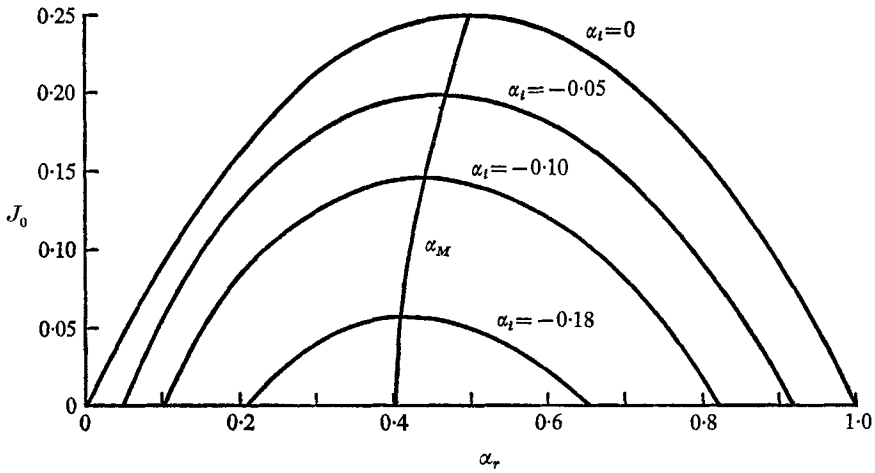

FIGURE 2. Curves of constant spatial growth rate in the buoyant case.

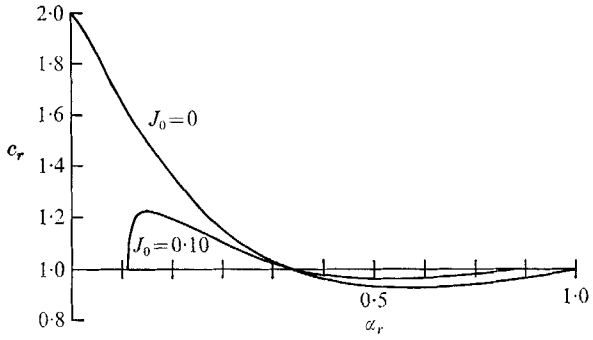

FIGURE 3. The variation of wave-speed with wave-number for spatially growing disturbances.

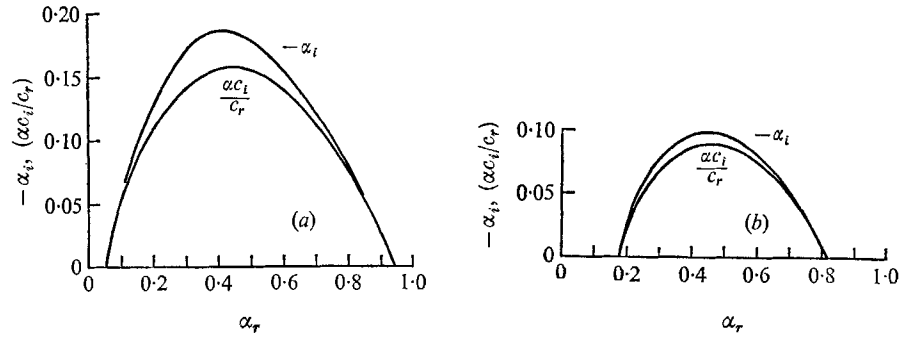

FIGURE 4. Comparison of spatial growth rates with $(\alpha c_i/c_r)$:
(a) $J_0 = 0{\cdot}05$, (b) $J_0 = 0{\cdot}15$.

In figure 4, we compare the calculated values of α_i to those predicted by use of the transformation $\alpha_i = -(\alpha_r c_i/c_r)$, $\alpha_r c_i$ being the temporal growth rate and $c_r = 1$, which appears to be the type of transformation which Scotti & Corcos (1969) used to relate their experimental results to Hazel's computed values of (αc_i). Using the results of Gaster (1962), it would be more precise to divide by the group velocity, rather than the phase velocity, of the disturbances which grow with time, but these disturbances are non-dispersive so that the two velocities are equal. As the Richardson number increases, the error incurred through use of the above first-order relation for α_i diminishes because α_i itself is diminishing and, as figure 3 indicates, the dispersion is rather weak over much of the wave-number range. The exception occurs at the lower cut-off wave-number, where Gaster's method would appear to be inapplicable due to the fact that the frequency is not an analytic function of the wave-number in the Kelvin–Helmholtz limit. At any rate, the numerical analysis always gives higher spatial growth rates than those obtained by the use of the approximate relation. From figure 3 of Scotti & Corcos (1969), one can see that the experimental results lie below the predicted growth rates, a discrepancy which clearly cannot be explained on the basis that only an approximate relation for the spatial growth rate was employed.

4. The inertial case

In the large Froude number limit, we set $J_0 = 0$ and take $\beta \sim O(1)$. Miles (1961) has shown, by considering the variation of the Reynolds stress, that in the case of a neutral mode

$$(\overline{\rho}\overline{u}')'_c = 0, \tag{4.1}$$

where the subscript c designates the point $\overline{u} = c$. The condition (4.1), in conjunction with (2.2), leads to the result that neutral solutions are regular in the inertial limit. Furthermore, (4.1) provides an explicit relationship between c and β in the case of a neutral mode. Thus, for Hølmboe's model, we obtain

$$c = 1 + \frac{1}{\beta} \pm \left(1 + \frac{1}{\beta^2}\right)^{\frac{1}{2}}. \tag{4.2}$$

By considering the limit $\beta \to 0$, it is clear that the $(+)$ sign is to be associated with $\beta < 0$ and the $(-)$ sign with $\beta > 0$. In either case, we note, in contrast to the result of Menkes, that the wave speed approaches the maximum or minimum mean flow velocity only as $|\beta| \to \infty$. This is directly associated with the result, to be discussed presently, that the flow cannot be rendered stable for any finite β.

Using (4.2), the governing equations (2.12)–(2.15) have been solved numerically to obtain the neutral curve and curves of constant c_i for temporally growing disturbances. These are displayed in figure 5. As $\beta \to 0$, the known results for homogeneous flow are duplicated and, for finite β and $\alpha \to 0$, the Kelvin–Helmholtz result

$$c_i = \left\{\frac{\overline{u}(\infty) - \overline{u}(-\infty)}{\overline{\rho}(\infty) + \overline{\rho}(-\infty)}\right\} [\overline{\rho}(\infty)\,\overline{\rho}(-\infty)]^{\frac{1}{2}} = \operatorname{sech}\beta \tag{4.3}$$

is obtained.

Hence, in contrast to the result of Menkes, the flow is unstable for all finite β. Although the range of unstable wave-numbers increases, one would say that the overall effect of density variation is stabilizing because, as figure 6 indicates, the maximum growth rate for any β is less than that which occurs in the homogeneous case. This conclusion changes, however, when we consider spatially growing disturbances, as figure 7 indicates. In that case, both the range of unstable wave-numbers and the maximum growth rate for $\beta > 0$ can be greater than for homogeneous flow. An absolute maximum in the spatial amplification factor is achieved for $\beta \cong 1{\cdot}75$ and is approximately 1·64 times the amplification factor for homogeneous flow. Ultimately, for very high β, it appears that reduced growth rates might occur but, for moderate β, it appears reasonable to state that the flow is destabilized when the lighter fluid has the higher velocity and stabilized, as far as the growth rate is concerned, when it has the lower velocity (as is apparent from the results for $\beta < 0$).

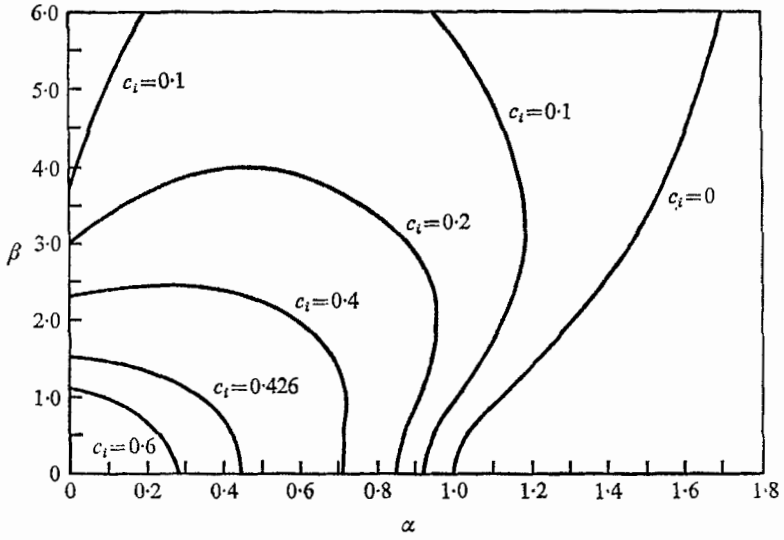

FIGURE 5. Curves of constant c_i for the inertial case.

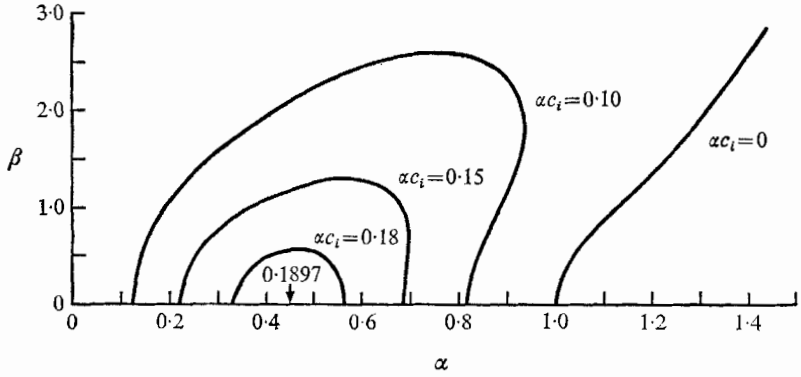

FIGURE 6. Curves of constant temporal growth rate for the inertial case.

The same general trends have been observed experimentally by Tombach (1969). A more detailed experimental investigation is currently being carried out at the California Institute of Technology by Professor Roshko and Dr R. Davey (see Davey 1971). While revising the present paper, the authors received a report by Gropengiesser (1969), in which the stability of a mixing layer in a compressible fluid, between streams of different velocity and temperature, was investigated. For low Mach numbers, the same trend in spatial growth rate as observed here was obtained, although it is unclear from Gropengiesser's results that a temperature ratio for maximum instability exists. For high free-stream Mach numbers,

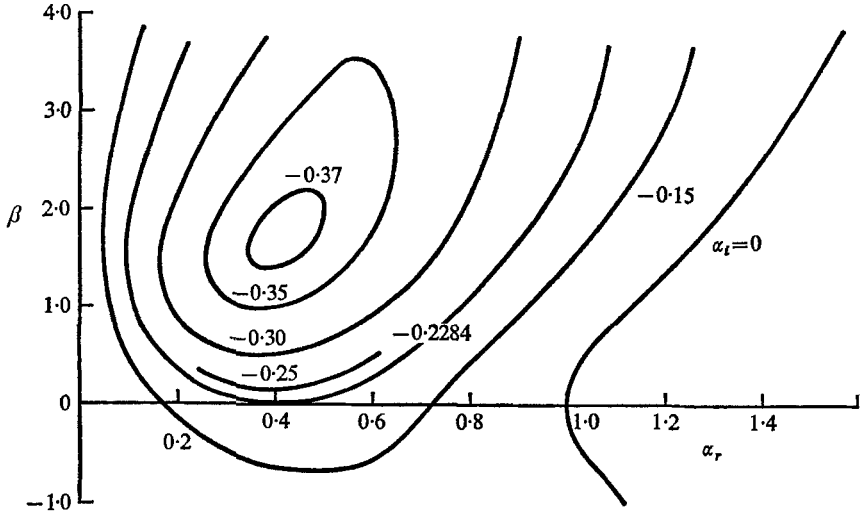

FIGURE 7. Curves of constant spatial growth rate for the inertial case ($-\alpha_i = 0{\cdot}3741$ for $\beta = 1{\cdot}75$, $\alpha_r = 0{\cdot}42$).

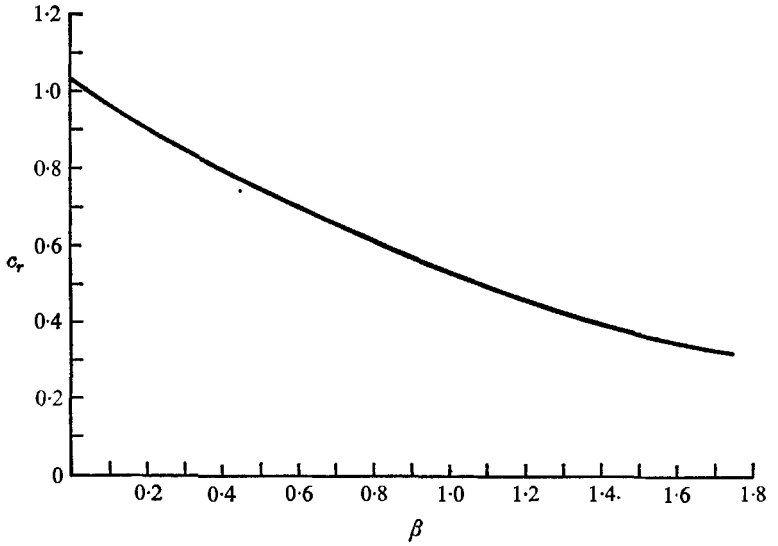

FIGURE 8. The variation of wave speed with β for the fastest spatially growing disturbances in the inertial case.

however, the trend is reversed. Because the shear-layer model is pertinent to the jet stability problem when the width of the jet is large in comparison to a typical wavelength, the results have importance in view of the argument of Berman & Ffowcs Williams (1970) that, in order to reduce jet noise, transition to turbulence should take place as rapidly as possible.

The reason for the enhanced amplification rate in the spatial growth case appears to be due simply to the decrease in the wave velocity for the wave of maximum amplification, as indicated in figure 8. The energy production term, in the energy equation for a disturbance, involves both the density and the shear of the mean flow. Over a certain range of positive β, it appears that the decrease in the shear in the 'critical layer' region, which is shifted downwards, can be compensated by the increase in density there. On the other hand, the rate at which the disturbance energy increases undergoes the following transformation, from the temporally to spatially amplified situation,

$$\frac{\partial}{\partial t}\iint \bar{\rho}(u^2+v^2)\,dx\,dy \rightarrow \frac{\partial}{\partial x}\iint \bar{\rho}\bar{u}(u^2+v^2)\,dx\,dy, \tag{4.4}$$

where the integrals are to be taken over the unbounded y domain and a wavelength. Because, for our model, $\bar{u}$ decreases more rapidly than $\bar{u}'$ for $|y| \ll 1$, it seems plausible to expect higher spatial amplification rates in order to strike a balance.

In conclusion, it should be pointed out that the results of Menkes are probably meaningful to a situation when the scale of the density layer is much larger than that of the velocity layer, although they are meaningless for the case of disturbances whose wavelengths are large in comparison to the scale of either layer for a realistic situation. Hence, the inertial stability problem for a heterogeneous shear flow is sensitive to the various scales involved, which is certainly also true for the buoyant case (cf. Hazel 1969).

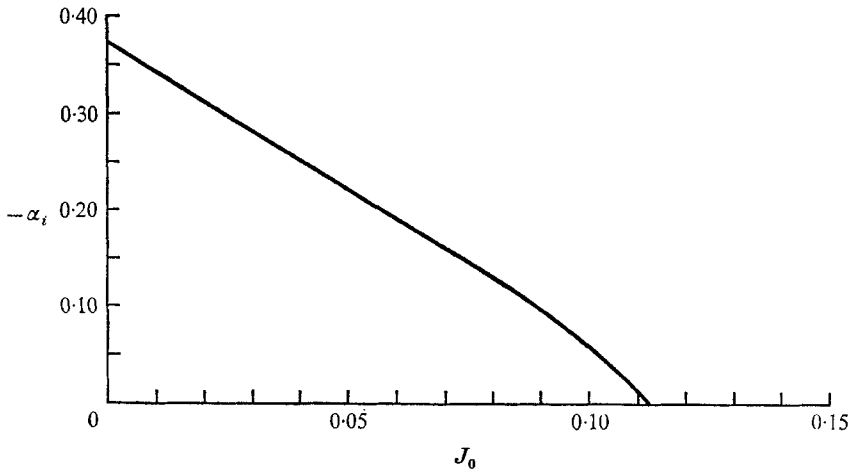

FIGURE 9. The effect of buoyancy upon the growth rate of the most unstable wave in the inertial case ($\alpha_r = 0{\cdot}42$, $\beta = 1{\cdot}75$).

5. The combined case

As pointed out in § 1, when both buoyancy and inertial effects are present, the flow must become stable as the minimum local Richardson number approaches $\frac{1}{4}$. In figure 9, we see how the spatial growth rate of the disturbance which is most unstable in the high Froude number limit decreases as the overall Richardson number increases. Because the value of the most unstable wave-number is relatively insensitive to variations in Froude number, these results are representative of the general case. The wave is stable when $J_0 = 0{\cdot}112$, corresponding to a local Richardson number $J_c = 0{\cdot}212$ (the wave velocity varied only from 0·320 to 0·316 as J_0 was increased from zero to 0·11). From figure 1, we note that this is a somewhat smaller value of the local critical Richardson number than occurs in the buoyant case ($\beta \to 0$), which indicates that the interaction of buoyancy and inertial density variations is rather involved.

Support for this work was given to one of us (R. E. K.) by the National Science Foundation (GK-4213).

REFERENCES

BERMAN, C. H. & FFOWCS WILLIAMS, J. E. 1970 *J. Fluid Mech.* **42**, 151.

DAVEY, R. F. 1971 Ph.D. thesis, California Institute of Technology.

DRAZIN, P. G. 1958 *J. Fluid Mech.* **4**, 214.

DRAZIN, P. G. & HOWARD, L. N. 1961 *Proc. Am. Soc. Civil Engrs (E.M. Div.)* **87**, 101.

DRAZIN, P. G. & HOWARD, L. N. 1966 *Adv. Appl. Mech.* **9**, 1.

GASTER, M. 1962 *J. Fluid Mech.* **14**, 222.

GROPENGIESSER, H. 1969 *Deutsche Versuchsanstalt für Luft-und Raumfahrt (DLR) Res. Rep.* (FB), 69–25.

HAZEL, P. 1969 Ph.D. thesis, Cambridge University.

HOWARD, L. N. 1961 *J. Fluid Mech.* **10**, 509.

KELLY, R. E. & MASLOWE, S. A. 1970 *Studies in Appl. Math.* **49**, 301.

MCLAFFERTY, G. H. 1968 *J. Spacecraft and Rockets*, **5**, 1121.

MASLOWE, S. A. & THOMPSON, J. M. 1971 *Phys. Fluids*, **14**, 453.

MENKES, J. 1959 *J. Fluid Mech.* **6**, 518.

MICHALKE, A. 1965 *J. Fluid Mech.* **23**, 521.

MILES, J. W. 1961 *J. Fluid Mech.* **10**, 496.

SCOTTI, R. S. 1969 Ph.D. thesis, University of California, Berkeley.

SCOTTI, R. S. & CORCOS, G. N. 1969 *Radio Science*, **4**, 1309.

THORPE, S. A. 1969 *J. Fluid Mech.* **36**, 673.

TOMBACH, I. H. 1969 Ph.D. thesis, California Institute of Technology.